

3 General Theory of Transport in Silicon-Germanium Alloys

Ignoring doping for the moment, there are two ways in which an alloy layer may be incorporated within a heterostructure. In a pseudomorphic structure (such as that described in Figure 3.1) a silicon-germanium alloy is grown directly on pure silicon. (It is normal practice not to grow the alloy directly onto the silicon substrate but to deposit a few hundred nanometres of pure silicon first.) The alloy layer is then generally capped by more pure silicon (there are issues regarding the oxidization of a silicon-germanium alloy¹). The alloy layer will match its lattice constant to that of the pure silicon, provided it is not too thick, the germanium concentration is not too high, or the growth temperature is not too high. For this reason, whilst pseudomorphic structures are generally simple to grow, they are generally limited to low germanium concentrations and thin alloy layers.

Alternatively, to allow for greater flexibility regarding thicker alloys with higher germanium concentrations or pure silicon under tensile strain (for electron channels, see Chapter 6) a virtual substrate may be grown. A buffer layer of alloy is grown and allowed to relax, and then the active channels are grown on this. The germanium concentration within the buffer may be graded to increase upwards, but is generally constant for the few hundred nanometres below the active channel. It is important to ensure that the buffer layer is fully relaxed (by growing it at a high enough temperature) and that the defects are not migrating up into the active channel.²

3.1 Principle Advantages In Using A Silicon-Germanium Heterostructure

There are three principle advantages to using a silicon-germanium heterostructure as opposed to a plain silicon-silicon dioxide (Si/SiO₂) system, arising from the lower effective mass, the possibility of band-structure engineering, and the energy band splitting in strained layers.

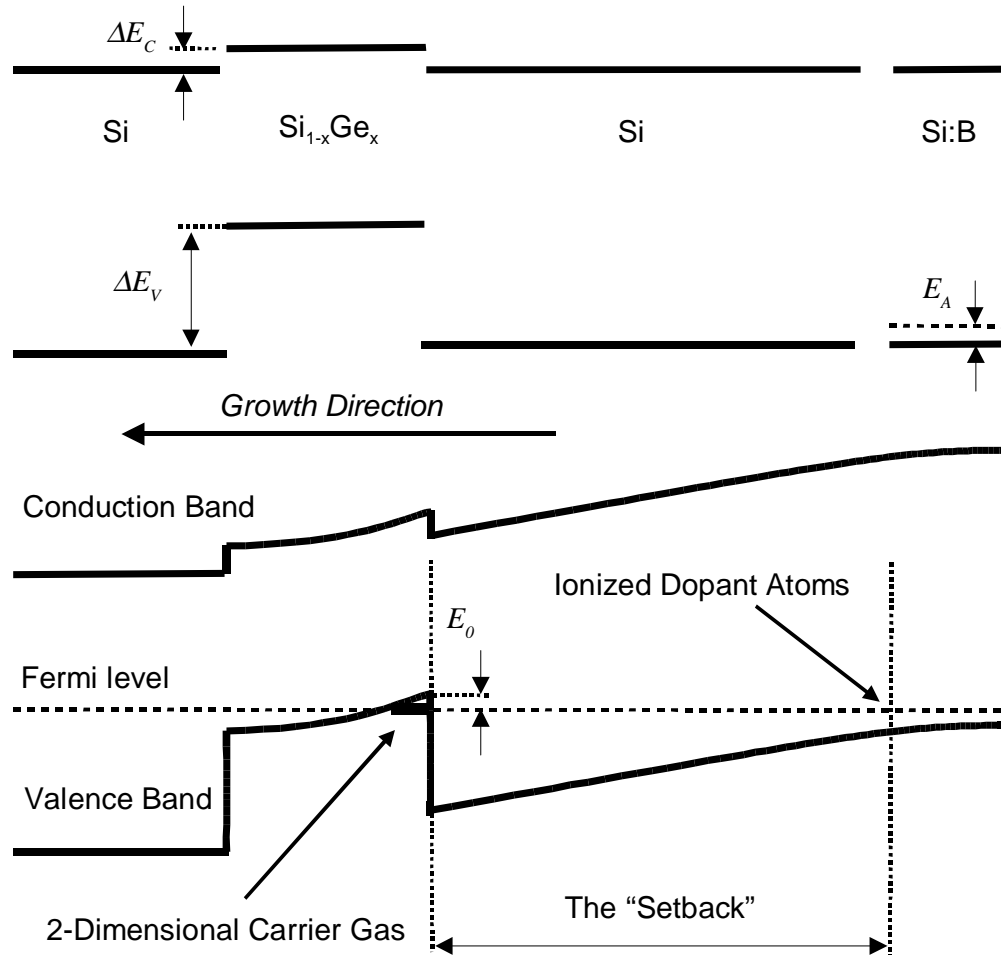


Figure 3.1 A schematic band profile of an inverted, pseudomorphic structure which shows how a 2-dimensional carrier gas (in this case, of holes) is formed. When brought together, dopant atoms ionize and charge accumulates at the nearest heterointerface.

3.1.1 Effective Mass

The mobility of electron and holes is inversely proportional to their effective mass (Equation 3.3) and the effective mass of holes is generally greater than that of electrons: some bulk properties of common semiconducting materials are summarized in Table 3.1.

	Ge	Si	GaAs
m_e^*/m_e	0.22	0.33	0.067
m_h^*/m_e	0.29	0.55	0.62
$\mu_e/cm^2V^{-1}s^{-1}$	3900	1500	8500
$\mu_h/cm^2V^{-1}s^{-1}$	1900	450	400

Table 3.1 Transport properties of some bulk semiconductors at 300K³

However, the effective mass of holes in bulk germanium is smaller than in almost any other semiconducting material and in fact at room temperature the mobility of holes in bulk germanium ($1900cm^2V^{-1}s^{-1}$) exceeds that of electrons in bulk silicon ($1500cm^2V^{-1}s^{-1}$). Therefore, it might be expected that sandwiching a layer of germanium, or at least a layer of germanium-rich alloy, between layers of silicon to use as a p-channel would be advantageous.^{3,4,5,6}

3.1.2 Band-Gap Engineering

The band-gap of germanium is smaller than that of silicon and so, by varying the concentration of germanium in the strained (active) layer* relative to that of the material it is lattice-matched to (either pure silicon in the case of a pseudomorphic system or an alloy in the case of a virtual substrate system) then offsets in the valence and conduction bands arise.⁷ The valence-band maximum is always in the material with the higher germanium concentration independently of which is the strained layer; for pseudomorphic systems where pure silicon is the substrate then the valence band offset is predicted to rise almost linearly to over 0.7eV for an active channel of pure, fully

* The band structure remains silicon-like (six conduction-band minima) for concentrations of germanium up to 85%, and is germanium-like (eight conduction-band minima) beyond this as far as the bulk unstrained alloy is concerned.

strained germanium.^{7,8} The conduction-band offset is less certain: if the active channel contains less germanium than the substrate (and is therefore under tensile strain) then the minimum in the conduction band will be in the active channel: a maximum offset of over 0.5eV is reached for pure silicon on a virtual substrate which is 85% germanium. However, if the active channel contains more germanium than the substrate then the conduction-band offset is almost always less than the error in the calculations.^{7,8} If the conduction-band minimum and the valence band maximum are both located within the strained layer then the band alignment is designated Type I, if one or the other resides in the substrate material then the band alignment is designated Type II.^{7,8}

If a layer of material either above (“normal”) or below (“inverted”) the active layer is doped, then the impurities supply carriers which diffuse into the active channel and are confined there in the triangular quantum well defined by the band offset and their own electrostatic potential to form a 2-dimensional carrier gas. The carriers are then free to move without being directly scattered by the ionized dopant impurity atoms.^{8,9,10,11} A schematic example of a band profile for an inverted, pseudomorphic structure (such as will be investigated in Chapters 5 and 7) at $T \ll T_F$ is shown in Figure 3.1.

3.1.3 Strain

The in-plane strain itself generates an anisotropic structure which breaks the conduction and valence band directional degeneracies. In silicon the 6 degenerate conduction band Δ minima are split into a set of 2 in the growth direction and a set of 4 in the plane. Under tensile strain, the former are at the lower energy, which greatly reduces intervalley scattering.⁸ In compressively-strained $\text{Si}_{1-x}\text{Ge}_x$ the light and heavy hole bands are split, substantially lowering the heavy hole mass to below that of the light holes with the heavy hole band lying lowest in energy. This reduces both the intersubband and intrasubband scattering.⁸ Generally, when band profiles are drawn, as in Figure 3.1, the “Valence band” and “Conduction band” energies each show only the $k_x=k_y=0$ point of the band which is lowest in energy.

3.2 The 2-Dimensional Carrier Gas

Figure 3.1 is a schematic band profile of a pseudomorphic, inverted p-channel heterostructure. The upper panel shows the components of the system (from right to left as grown: boron-doped silicon, intrinsic silicon, fully strained alloy) and the lower panel shows how the energy bands arrange when an equilibrium is reached. Acceptor atoms at the edge of the dopant slab ionize,* and these free holes form a 2-Dimensional Hole Gas (2DHG) at the heterointerface. (In this system, there are no free charges in the system from, for example, contamination of the supposedly undoped layers. Such “depletion charge” N_{Depl} will be incorporated if necessary, in later chapters.) The 2DHG is examined more closely in Figure 3.2. The electric field between the heterointerface and the dopant slab is directly proportional to the charge density in the 2DHG:

$$F = \frac{e}{\epsilon_0 \epsilon_r} (n_S + N_{Depl}) = \frac{e n_S}{\epsilon_0 \epsilon_r} \quad \text{if } N_{Depl} = 0 \quad 3.1$$

The system is drawn with flat bands in the cap layer effectively meaning that there is no free charge anywhere else. Often, as will be seen in later chapters, the formation of an inversion layer at the top of the silicon cap layer is an important consideration.

A triangular quantum well is formed in the valence band. Motion of carriers is constrained completely in the growth direction but free (within the usual effective-mass assumption) perpendicular to the growth direction. It is generally the case that only the ground state of this quantum well is populated (up to the Fermi Energy E_F , as shown in the lower panel of Figure 3.2) since the spacing between the energy levels is of the order of tens of electronvolts for sheet densities ($\sim 10^{12} \text{cm}^{-2}$) comparable to those discussed in later chapters. (In fact, the quantum well ceases to be approximately triangular on these energy scales.) The Fang-Howard approximation to the wavefunction in the ground state of this triangular well is shown¹²

* It is assumed that the dopant depletion width is small enough to be neglected. For typical modulation doping doses, it is roughly 2nm.

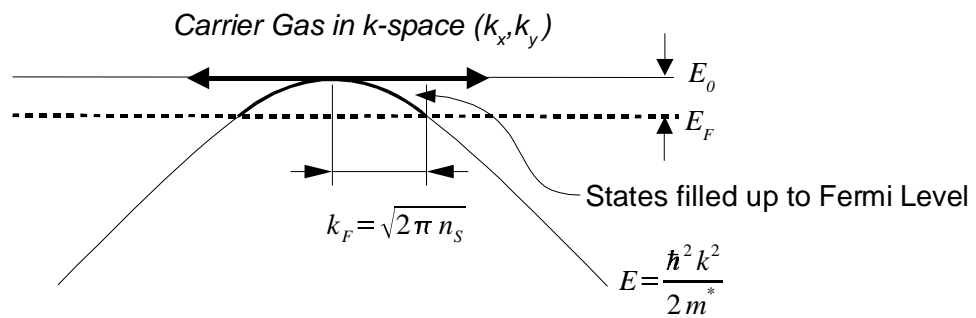
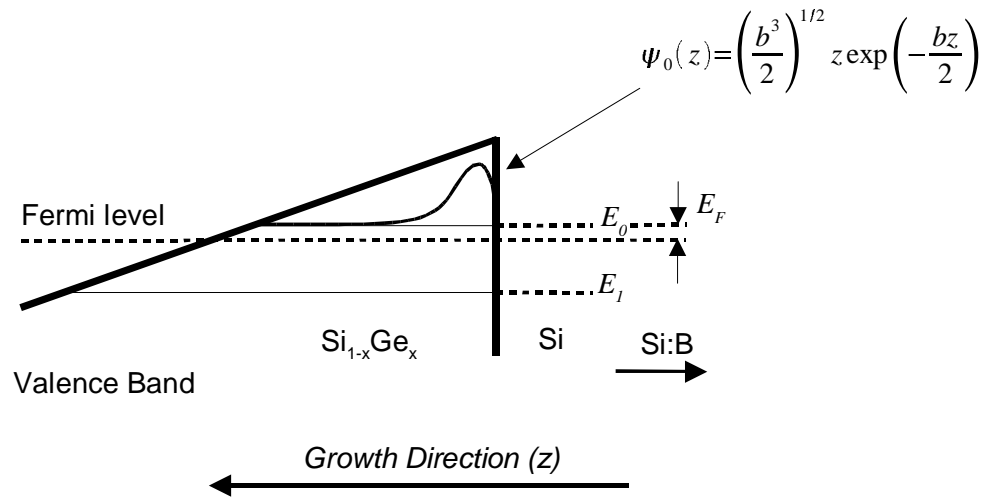


Figure 3.2 The upper panel gives a closer view of the heterointerface, where the 2DHG forms. E_0 and E_1 represent the two lowest quantum energy levels of the triangular potential well formed by the valence band. The simple Fang-Howard wavefunction is shown, which assumes that the vertical potential barrier is effectively infinite. The lower panel shows how the Fermi Energy E_F depends on the sheet density in the simplest case of constant, isotropic effective mass.

$$\psi_0(z) = \left(\frac{b^3}{2}\right)^{1/2} z e\left(-\frac{bz}{2}\right) \quad 3.2$$

where b is a variational parameter. This wavefunction assumes that the band offset at the heterointerface is infinite, so the probability density is zero at the interface itself. A realistic finite valence band offset would lead there to be a small, finite component to the wavefunction across the heterointerface, and this has implications for some of the scattering mechanisms which are discussed in the following section.

3.3 Scattering

By considering the rate of change of momentum of the charge carriers, the mobility (as defined in equation 4.1) is found to be related to the transport scattering time τ by¹³

$$\mu = \frac{e\tau}{m_*} \quad 3.3$$

Matthiesen's rule says that the total scattering rate is the sum of the scattering rates due to each of the processes operating within the material:¹³

$$\tau^{-1} = \frac{e}{\mu m_*} = \sum_i \tau_i^{-1} \quad 3.4$$

At finite temperature, Equation 3.3 becomes an integral which takes into account the energy dependence of the relaxation rates τ_i^{-1} .¹⁴ However, the qualitative result is the same: the mobility is essentially limited by the scattering mechanism with the highest relaxation rate. Scattering rates are generally calculated by considering the reaction of a charge-carrying particle to some sort of potential. This approach necessarily incorporates screening: a particular carrier sees not the potential itself, but rather the potential screened to some extent by the rest of the carrier gas.^{14,15,16} Some typical scattering mechanisms will be mentioned here, with more specific (and

mathematical) details to be presented in later chapters.

3.3.1 Impurities

Charge carriers may be scattered by impurities located at or close to the interface at which they are confined. This interface impurity scattering depends mainly on density of impurities at the interface and is stronger when the sheet density of the charge carriers is lower. (At the lowest sheet densities, multiple scattering becomes relevant and eventually the carrier gas becomes strongly localized.¹⁶) As sheet density increases, impurities are increasingly screened and the scattering effect is reduced.^{14,17,18}

3.3.2 Interface Roughness

The roughness of the interface at which the charge carriers are confined leads to scattering which depends on the depth of the fluctuations, and their characteristic correlation length. The strongest scattering occurs for deep fluctuations when the carrier density is such that the Fermi wavelength coincides with the fluctuation correlation length.^{14,19}

3.3.3 Alloy Effects

Alloy scattering and scattering from strain fluctuations may be blamed for the poor performance of heterostructures where the active channel is an alloy with roughly equal germanium and silicon concentrations. The first mechanism exists because even though the silicon-germanium alloy has a crystalline structure, whether a silicon or germanium atom occupies a particular lattice site is random. There is controversy regarding the strength of this mechanism.^{14,20} (Poor performance of structures which feature intermediate germanium concentrations may not be due to alloy scattering directly but due to issues regarding the growth of the heterostructures: low growth temperatures are needed to avoid the relaxation of the alloy as it is grown but lead to poor material with high crystal defect densities. Higher growth temperatures lead to the formation of germanium-rich islands on the growth surface and eventually result in a

material with uneven germanium distribution and an undulating interface.²¹) The second mechanism is induced by deformation associated with interface roughness.

3.3.4 Phonons

The acoustic phonon scattering relaxation rate is directly proportional to temperature and is related to material and physical constants rather than electronic parameters. In a confined geometry, optical phonon scattering should be considerably weaker provided that only a single subband is occupied.^{4,20} In any case, phonon scattering is not relevant unless the lattice temperature is greater than the Fermi temperature and the carrier gas becomes nondegenerate,⁴ which for a 2-dimensional carrier gas with a circular Fermi line and a constant effective mass is:

$$T_F = \frac{E_F}{k_B} = \frac{1}{k_B} \frac{\hbar^2 k_F^2}{2m^*} = \frac{\hbar^2 \pi n_S}{k_B m^*} \quad 3.5$$

These analyses have generally neglected the interactions between carriers in the gas, and other effects which are most relevant at very low temperatures or high magnetic fields, and will be introduced in Chapter 4.

- 1 P. W. Li and E. S. Yang, *SiGe gate oxide prepared at low-temperatures in an electron cyclotron resonance plasma*, Applied Physics Letters **63** (21) 2938-2940 (1993)
- 2 D. C. Houghton, *Strain relaxation kinetics in $Si_{1-x}Ge_x/Si$ heterostructures*, Journal of Applied Physics **70** (4) 2136-2151 (1991)
- 3 S. M. Sze, *Semiconductor Devices: Physics and Technology*, Wiley 1985.
- 4 B. Laikhtman and R. A. Kiehl, *Theoretical hole mobility in a narrow Si/SiGe quantum well*, Physical Review B **47** (16) 10515-10527 (1993)
- 5 T. E. Whall, A. D. Plews, N. L. Matthey, P. J. Phillips and U. Ekenberg, *Effective mass and band nonparabolicity in remote doped $Si/Si_{0.8}Ge_{0.2}$ quantum wells*, Applied Physics Letters **66** (20) 2724-2726 (1995)
- 6 T. E. Whall, A. D. Plews, N. L. Matthey and E. H. C. Parker, *Hole effective mass in remote doped $Si/Si_{1-x}Ge_x$ quantum wells with $0.05 \leq x \leq 0.3$* , Applied Physics Letters **65** (26) 3362-3364 (1994)
- 7 M. M. Rieger and P. Vogl, *Electronic-band parameters in strained $Si_{1-x}Ge_x$ alloys on $Si_{1-y}Ge_y$ substrates*, Physical Review B **48** (19) 14276-14287 (1993)
- 8 F. Schäffler, *High-mobility Si and Ge structures*, Semiconductor Science and Technology **12** 1515-1549 (1997)
- 9 M. A. Sadeghzadeh, C. P. Parry, P. J. Phillips, E. H. C. Parker and T. E. Whall, *Issues on the molecular-beam epitaxial growth of p-SiGe inverted-modulation-doped structures*, Applied Physics Letters **74** (4) 579-581 (1999)
- 10 T. E. Whall and E. H. C. Parker, *SiGe – heterostructures for CMOS technology*, Thin Solid Films **367** 250-259 (2000)
- 11 G. Abstreiter, *Electronic Properties of Si/SiGe/Ge Heterostructures*, Physica Scripta, **T68**, 61-71 (1996)
- 12 T. Ando, A. B. Fowler and F. Stern, *Electronic properties of two-dimensional systems*, Reviews of Modern Physics **54** (2) 437-621 (1982)
- 13 J. S. Blakemore, *Solid State Physics Second Edition*, Cambridge University Press 1985.
- 14 R. J. P. Lander, M. J. Kearney, A. I. Horrell, E. H. C. Parker, P. J. Phillips and T. E. Whall, *On the low-temperature mobility of holes in gated oxide Si/SiGe heterostructures*, Semiconductor Science and Technology **12** 1064-1071 (1997)
- 15 A. D. Plews, N. L. Matthey, P. J. Phillips, E. H. C. Parker and T. E. Whall, *Screening phenomena in $Si/Si_{1-x}Ge_x$ quantum wells*, Semiconductor Science and Technology **12** 1231-1234 (1997)
- 16 M. J. Kearney and A. I. Horrell, *An analysis of the mobility of holes in p-type SiGe quantum wells using multiple scattering theory*, Semiconductor Science and Technology **14** 211-214 (1999)
- 17 C. J. Emeleus, T. E. Whall, D. W. Smith, R. A. Kubiak, E. H. C. Parker and M. J. Kearney, *Scattering mechanisms affecting hole transport in remote-doped Si/SiGe heterostructures*, Journal of

Applied Physics **73** (8) 3852-3856 (1993)

18 T. Tezuka, T. Hatakeyama, S. Imai, N. Sugiyama and A. Kurobe, *Mobility modulation of two-dimensional hole gas in a p-type Si/SiGe modulation doped heterostructure by back-gating*, Semiconductor Science and Technology **13** 1477-1479 (1998)

19 A. Yutani and Y. Shiraki, *Transport properties of n-channel Si/SiGe modulation-doped systems with varied channel thickness: effect of the interface roughness*, Semiconductor Science and Technology **11** 1009-1014 (1996)

20 M. J. Kearney and A. I. Horrell, *The effect of alloy scattering on the mobility of holes in a $Si_{1-x}Ge_x$ quantum well*, Semiconductor Science and Technology **13** 174-180 (1998)

21 T. J. Grasby, C. P. Parry, P. J. Phillips, B. M. McGregor, R. J. H. Morris, G. Braithwaite, T. E. Whall, E. H. C. Parker, R. Hammond, A. P. Knights and P. G. Coleman, *Technique for producing highly planar Si/SiO_{0.64}Ge_{0.36}/Si metal-oxide-semiconductor field effect transistor channels*, Applied Physics Letters **74** (13) 1848-1850 (1999)